SIMULATED PROPAGATION OF CARDIAC ACTION POTENTIALS

GREGORY H. SHARP, *Department of Physiology, Duke University, Durham, North Carolina 27710*
RONALD W. JOYNER, *Department of Physiology and Biophysics, University of Iowa, Iowa City, Iowa 52242 U.S.A.*

ABSTRACT We have used numerical methods for solving cable equations, combined with previously published mathematical models for the membrane properties of ventricular and Purkinje cells, to simulate the propagation of cardiac action potentials along a unidimensional strand. Two types of inhomogeneities have been simulated and the results compared with experimentally observed disturbances in cardiac action potential propagation. Changes in the membrane model for regions of the strand were introduced to simulate regions of decreased excitability. Regional changes in the intercellular coupling were also studied. The results illustrate and help to explain the disturbances in propagation which have been reported to occur at regions of decreased excitability, regions with changing action potential duration, or regions with changing intercellular coupling. The propagational disturbances seen at all of these regions are discussed in terms of the changing electrical load imposed upon the propagating impulse.

INTRODUCTION

The normal sequence of cardiac excitation, as well as the changes produced by regional injury and premature excitation, are exceedingly complex, but must have a physical basis in the interrelationships of two sets of properties. We will refer to these as the active properties (the voltage and time dependent membrane currents which give rise to the action potential) and the passive properties (the membrane capacitance, the electrical coupling between cells, and the geometry of interconnections). It is clear that both sets of properties vary in different regions of the heart and also that they are changed by ischemia and drug actions, including the normal autonomic activity. However, to the extent that these properties can be defined for a particular region of the heart, under a particular set of conditions, it is possible to integrate our knowledge of these individual properties into a model which should then be able to simulate the observed process of action potential propagation.

The measurement of the passive electrical properties of cardiac muscle has been extremely difficult due to the small size of the cells and the multidimensional nature of the cardiac syncytium (see review by Schanne and Ruiz-Ceretti, 1978). Capacitance measurements (Weidman, 1970; Lieberman et al., 1975) have indicated two components of membrane capacitance: 0.5–2 $\mu F/cm^2$ associated with the "exposed" surface membrane, and 10–12 $\mu F/cm^2$ Purkinje fibers, with area referred to external surface associated with the transverse

Please send reprint requests to Dr. Joyner.

tubular system and/or the membrane of narrow intercellular clefts (see Mobley and Page [1972] for a detailed anatomical analysis). Also, values of R_m (specific membrane resistivity, Ω cm^2) and R_i (equivalent resistivity of the core of a fiber strand, Ω cm) have varied enormously with tissue type and methodology, with a general range of 1,000 to 4,000 Ω cm^2 for R_m of vertebrate systems.

There appear to be significant variations in the passive parameters in different regions of the heart (Challice, 1971; Pollack, 1976) and in a specific region there may be directional variations in the coupling resistance, reflected in different values of R_i for different fiber orientations (Woodbury and Crill, 1961; Clerc, 1976). Recent evidence has also indicated that the coupling resistance between cardiac cells may be increased by changes in the intracellular concentrations of sodium and calcium (Weingart, 1975; De Mello, 1976).

The establishment of a model for the membrane properties which give rise to the action potential has been extremely controversial. The application of the voltage clamp technique to cardiac tissue, either with two microelectrodes (Deck et al., 1964) or the sucrose gap (Rougier et al., 1968), compared with the axial wire voltage clamp of the squid giant axon (Hodgkin and Huxley, 1952), is complicated by spatial voltage inhomogeneity, large distributed series resistance, and a loss of control during the initial inward current phase (Johnson and Lieberman, 1971; Atwell and Cohen, 1977). The two models used in this paper represent syntheses of voltage clamp experiments by many investigators on Purkinje fibers (McAllister, Noble, and Tsien [1975] "MNT") and ventricular muscle fibers (Beeler and Reuter [1977] "BR"). In each case, the models represent an extension of the Hodgkin and Huxley (1952) formalism of ionic conductances which are functions of voltage and time, although significant new features are included to recreate the voltage clamp data and the shape of the membrane action potential. Some of these differences are the use of instantaneously nonlinear current-voltage relationships for some ionic currents, and, in the BR model, variations in the equilibrium potential for calcium with the calculated changes in the internal calcium concentration. While it is understood that quantitative and, perhaps, qualitative changes in these models will be necessary as further improvements in the voltage clamp technique are made, the models do recreate many of the electrical phenomena associated with ionic concentration changes, drug effects, and changes in the rate of stimulation.

Previous work on simulating the propagation of cardiac action potentials has been done with drastic simplifications in either the membrane model used or the cable properties of the cardiac syncytium. Models of wavefront propagation through a sheet of tissue have used a coupled array of logic elements with variable states (Wiener and Rosenblueth, 1946; Moe et al., 1964), or more recently with a two-dimensional cable model for the sheet but the Hodgkin-Huxley axon model for the membrane properties (Joyner et al., 1975). Propagation along a one-dimensional fiber has been simulated with analytical solutions for particular boundary conditions (Terry et al., 1972) or by implementation of an electrical cable using multistate logic elements (van Capelle and Janse, 1976).

Lieberman et al. (1973) have done simulations with a one-dimensional cable model in which the longitudinal resistivity and membrane properties were varied along the strand. The membrane model used in their work consisted of a sodium conductance from the H-H equations and a constant potassium conductance. The major difference in the present work is the incorporation of published membrane models which generate a "complete" cardiac action

potential, although (see Discussion) the part of these models which has the greatest uncertainty is the transient sodium conductance.

Previous work on simulating the propagation of nerve action potentials has led to significant understanding of the mechanisms of conduction failure at regions of changing membrane properties or changing geometry (Cooley and Dodge, 1966; Schauf and Davis, 1974; Goldstein and Rall, 1974; Westerfield et al., 1978), and the dependence of conduction velocity on the various components of the nerve model (Brill et al., 1977; Moore et al., 1978). Understandably, nerve modeling has been greatly facilitated by the simple equivalent circuit model required and the early establishment of a quantitative model for the active membrane properties. In this paper we present a method for simulating propagation along a strand of cardiac tissue, using the MNT or BR model as a description of the membrane properties. We restrict the present work to a one-dimensional simulation, even though the methods for simulating a sheet of cells have already been presented (Joyner et al., 1975), because of the large amount of computations needed for the two-dimensional case, and also because the one-dimensional simulations correspond well to experiments on strips of tissue and also illustrate the basic mechanisms involved in propagational disturbances in more complex systems.

METHODS

The simulation of action potential propagation requires the simultaneous simulation of two types of models. The first model is that of the membrane properties which produce an action potential in an isopotential membrane region, stated as a set of differential equations relating individual membrane currents as functions of voltage and time. The second model is an equivalent circuit representation of the cable properties of the tissue. We used an equivalent cable with the following properties:

R_i = specific axial resistivity	(200 Ω cm)
C_m = specific membrane capacitance	(1 uF/cm^2)
ΔX = spatial increment	(0.00625–0.025 cm)
Δt = time increment	(5–10 μs)
a = fiber radius (cell radius)	(2.5–12.5 μm)

For a passive cable with membrane resistivity R_m (Ω cm^2), we can derive length specific parameters as:

$$r_i = R_i/(\pi a^2)$$
$$c_m = C_m(2\pi a)$$
$$r_m = R_m/(2\pi a)$$

and, for each segment, we can define

i_{ion} = ionic current per unit length (milliamperes per centimeter)
i_i = axial current (milliamperes)
i_m = total membrane current (milliamperes per centimeter).

If we let V_j^t be the membrane potential of segment j at time t, then we can derive a set of equations expressing the parameters $V_j^{t+\Delta t}$ as functions of V_j^t, the membrane currents, and the passive cable parameters. The method used here was developed by Crank and Nicholson (1947) and has been

previously applied to simulate action potential propagation in several tissues. In brief, the technique is to write the well known cable equation:

$$\frac{\partial^2 V}{\partial X^2} = r_i \left(C_m \frac{\partial V}{\partial t} + i_{ion} \right)$$

as a difference equation for each segment, using the time average (at t and at $t + \Delta t$) for the second central difference form of the spatial derivative. The result can be written as a set of equations (one for each segment of the cable):

$$b_j V_{j-1}^{t+\Delta t} + d_j V_j^{t+\Delta t} + a_j V_{j+1}^{t+\Delta t} = c_j,$$

where $K = \Delta t/[r_i c_m (\Delta X)^2]$,

$$\begin{aligned} a_j &= -K \\ b_j &= -K \\ d_j &= 2(1 + K) \\ c_j &= 2(1 + K)V_j^t + K(V_{j-1}^t + V_{j+1}^t) - 2\,\Delta t(i_{ion})/c_m. \end{aligned}$$

A detailed representation of the solution method and the extension of this form to include various boundary conditions, as well as spatial inhomogeneity in the passive parameters, has already been published (Joyner et al., 1978). In the present work we utilize this method so that, at each time step, we: (*a*) compute the total ionic current, i_{ion}, for each segment, using the MNT or BR model for the action potential properties; (*b*) use these currents and the values of V_j^t to compute the values of $V_j^{t+\Delta t}$; (*c*) plot and/or store the voltages and currents and then return to step *a* for the next time step.

Both the MNT and the BR model have been previously presented in detail. We present here only the solution method we used. The general form of the ionic currents for both models is (cf. Hodgkin and Huxley [1952]):

$$i_u = \bar{g}_u y z (V - E_u),$$

where $\bar{g}_u$ is a constant maximum conductance, E_u is the ionic equilibrium potential, and y and z are kinetic parameters defined as:

$$dy/dt = \alpha_y - (\alpha_y + \beta_y) y,$$

where α_y and β_y are functions of voltage. However, some of the specified currents have a slightly different form, e.g.:

$$i_x = \bar{i}_x \cdot x,$$

where x is a kinetic parameter similar to y and z above, but $\bar{i}_x$ represents a maximum current and is defined as a nonlinear function of voltage. Another feature of the BR model is that the slow inward current is treated as a calcium current for which the reversal potential, E_s, is not constant, but is continuously computed from:

$$E_s = -82.3 - 13.0287 \ln [\mathrm{Ca}]_i$$

and

$$\mathrm{d}[\mathrm{Ca}]_i/\mathrm{d}t = -10^{-7} i_s + 0.07(10^{-7} - [\mathrm{Ca}]_i).$$

The initial conditions for the models are very important. For the MNT model the initial conditions for the kinetic parameters are computed from:

$$y = \alpha_y/\alpha_y + \beta_y,$$

where the α's and β's are computed for an initial voltage of -80 mV. For the BR model, the initial conditions for a standard action potential are computed by first starting the model with initial conditions as described above for the MNT model and then doing a continuous simulation while pacing the model once per second until the action potential shape reaches a constant form. The standard initialization parameters are then the values of the kinetic parameters and $[Ca]_i$ corresponding to a time just before one of the periodic pacing stimuli. This procedure needs to be done only once for the standard model, since the initialization parameters can be simply set for subsequent simulations. The parameters were kindly furnished to us by Dr. Beeler (Mayo Clinic, Rochester, Minn.): $m = 0.01126$, $h = 0.9871$, $x = 0.0241$, $j = 0.9927$, $d = 0.0030$, $[Ca]_i = 0.792E\text{-}7$, $V = 84.35$, and $f = 1.0$.

The actual procedure used to integrate the kinetic parameters for both models was to store values of the α's and β's in a table for voltages from -100 mV to $+100$ mV in steps of 1 mV. This results in an enormous saving of computer time (~90%), as opposed to computing the α's and β's at every time step. Thus, the procedure used to calculate the ionic current for each segment at each time step was: (*a*) using the membrane potential, set values for the α's and β's as well as the $\bar{I}$ terms, using a linear interpolation between voltage steps; (*b*) integrate all kinetic parameters one time step; (*c*) calculate new $[Ca]_i$ and E_s (BR only); and (*d*) calculate and sum the individual ionic currents.

The computation time involved for a simulation of a 100 segment cable for 500 ms was ~1 h of central processing unit time on a VAX 11/780 computer (Digital Equipment Corp., Maynard, Mass.) (about 20 times longer on a PDP 11/34 with a floating point processor). The results were stored on the disk and then transferred to a PDP 11/34 computer (Digital Equipment Corp.) for plotting and generation of hard copies via a Tektronix 4014 graphics terminal (Tektronix, Inc., Beaverton, Oreg.).

RESULTS

Throughout this paper we will refer to the action potential generated in an isolated isopotential patch of membrane as a membrane action potential (MAP), and the action potential generated at one segment of the cable model as a propagated action potential (PAP). For the homogeneous cable the PAP for each segment closely resembles the MAP that would have resulted from isolating and stimulating a single segment of the cable. We will deal with two types of inhomogeneities in the cable model. In one type, the membrane model is the same for all segments, but the coupling resistance between adjacent segments is varied along the fiber. In the other type, some parameter of the membrane model (e.g., the maximum conductance of the slow inward current) is varied along the fiber. We can thus create regional inhomogeneities, or lesions, and investigate not only how the PAP of the modified segment is different from what the MAP for that segment would be, but also how the PAP is changed in other segments which have normal membrane properties and normal coupling resistance.

Membrane Action Potentials

Fig. 1 *A* shows the MAP generated by a brief stimulus to the BR membrane model. Curves labeled *a*, *b*, *c*, and *d* correspond to variations in the maximum conductance for the slow inward current, with scaling factors of 1.0 (*a*), 0.8 (*b*), 0.6 (*c*), and 0.4 (*d*). As expected, the rising phase of the MAP is not affected, but the plateau phase becomes much shorter as the slow inward current is decreased. Similar results were obtained by increasing the magnitude of the delayed outward current. Part *B* of the figure shows the MAP resulting from a brief stimulus (instantaneous jump of membrane potential from -80 mV to -50 mV) to the MNT model.

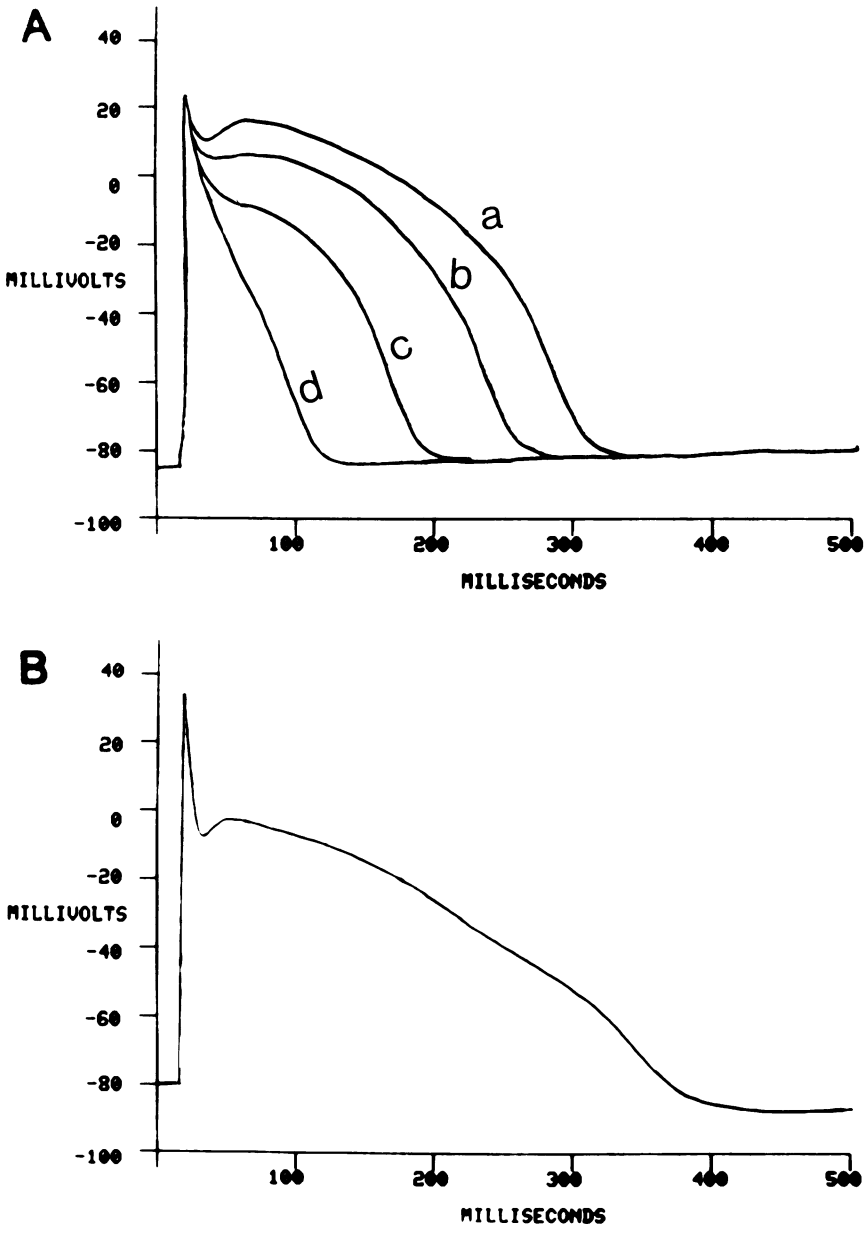

FIGURE 1 (*A*) Solutions for the BR action potential model for an isopotential cell. The slow inward current is scaled by 1.0 (*a*), 0.8 (*b*), 0.6 (*c*), or 0.4 (*d*). (*B*) Solution for the MNT action potential mode.

Propagation along a Homogeneous Cable Model

Fig. 2 *A* shows the PAP's recorded from a series of segments of a homogeneous cable, using the BR membrane model. The stimulation was applied to segment 1 and the PAP's shown are for segments 5–50 in increments of 5. The curves are shifted vertically for clarity, with the top curve corresponding to segment 5. It is apparent that the action potential propagates at a

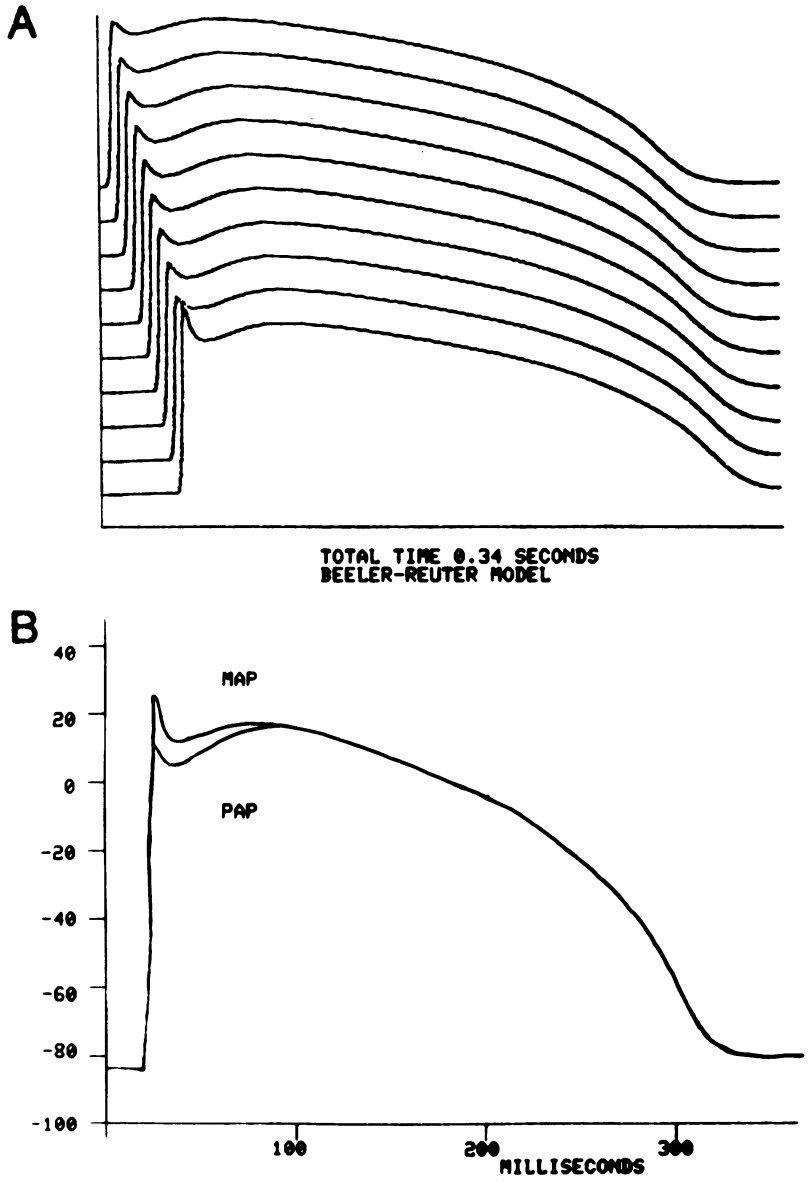

FIGURE 2 (*A*) A series of plots of voltage versus time for 10 segments (5, 10, 15 . . . 50) for a simulation of the BR model in a strand represented by 50 segments (ΔX = 250 μm). Stimulation occurred at segment 1. Curves are displaced vertically for clarity, with the top trace corresponding to segment 5. (*B*) The propagating action potential of segment 25 (from *A*) is superimposed with the isopotential result (MAP) showing the effects of the cable properties in the early part of the AP.

uniform conduction velocity and with no changes in shape along the fiber. However, as shown in Fig. 2 *B*, the PAP for this cable is not identical with the MAP for the BR model. There is a noticeable decrease in the spike amplitude but no change in the plateau shape or duration. Similar results were obtained for the MNT model (not shown), with a conduction velocity obtained for this cable (cell radius 2.5 μm, R_i = 200 Ω cm, C_m = 1 uF/cm^2) of 35 cm/s (BR)

and 73 cm/s (MNT). However, for a more realistic Purkinje cell diameter of 50 μm, the velocity was 231 cm/s. The resting membrane resistance of the BR model is ~5,000 Ω cm^2, giving a resting length constant of 0.6 mm for the fiber radius used in these simulations.

Spatial Inhomogeneity in Membrane Properties

As illustrated in Fig. 1 *A*, the action potential duration of the BR model MAP can be varied by scaling the magnitude of the slow inward current. Fig. 3 *A* shows the results of using a scale

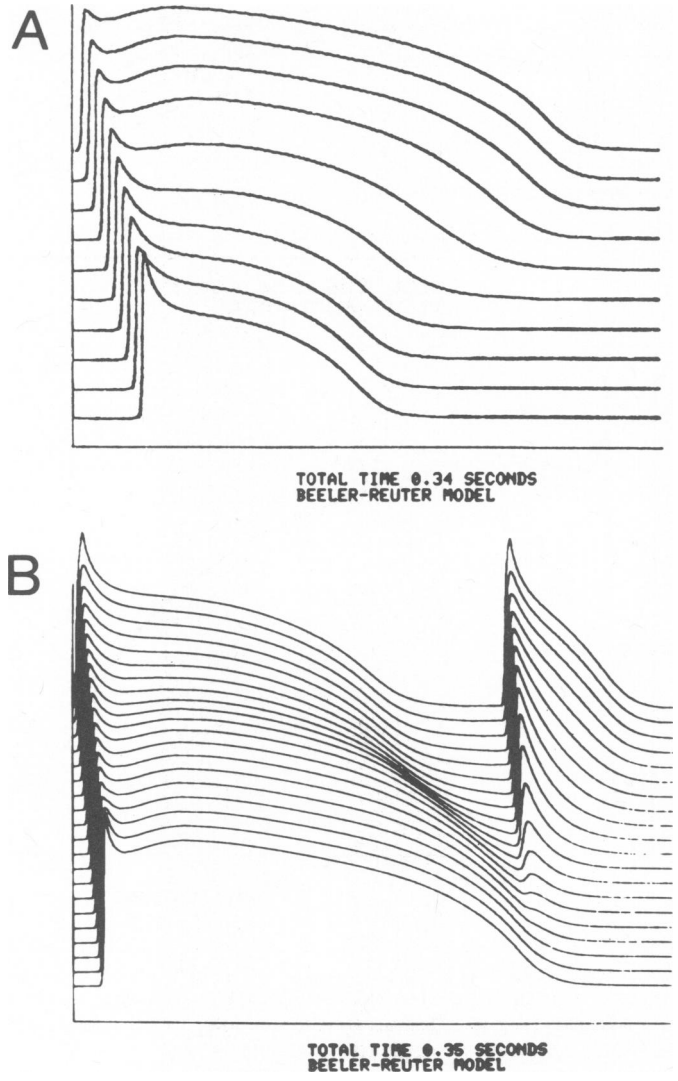

FIGURE 3 (*A*) A series of plots of voltage versus time for 10 segments (5, 10, 15 . . . 50 from top down) for a 50-segment cable in which the BR model has the slow inward current scaled by 1.0 (segments 1–25) or 0.6 (segments 26–50). ΔX = 250 μm. (*B*) A series of plots of voltage versus time for 20 segments (5, 10, 15 . . . 100 from top down) for a 100-segment cable (ΔX = 62.5 μm) in which the BR model has the slow inward current scaled by 0.1 for segments 1–50 and by 1.0 for segments 51–100. Both stimuli are applied to segment 1.

factor of 0.6 for this current for segments 25–50 of a 50 segment cable. The PAP's are plotted for segments 5–50 in increments of 5 as before. Even though the transition in membrane properties is made abruptly at segment 25, the PAP waveform shows an effect of this change at all segments, making it appear that a gradual transition in membrane properties was present. Similar results were obtained when this fiber was stimulated at segment 50. In either case, the electronic interactions during the plateau phase tend to obscure the abrupt nature of the transition in membrane properties. In Fig. 3 *B* we show the results for a 100 segment cable in which, for segments 1–50, the membrane model was changed by scaling the slow inward current by 0.1. As in part *A*, there is a gradual increase in action potential duration along the fiber; and, a second stimulus applied to segment 1, with a delay of 250 ms, initiates a second action potential which propagates decrementally and then fails as it reaches regions with increasing action potential duration.

To simulate a region of decreased excitability, we set $\bar{g}_{Na} = 0$ for a region of the cable. Fig. 4 shows the results for a 100 segment cable in which $\bar{g}_{Na} = 0$ for segments 51–56 (*A*), 51–54 (*B*), and 51–58 (*C*). For part *B*, the regional decrease in excitability produces changes in the

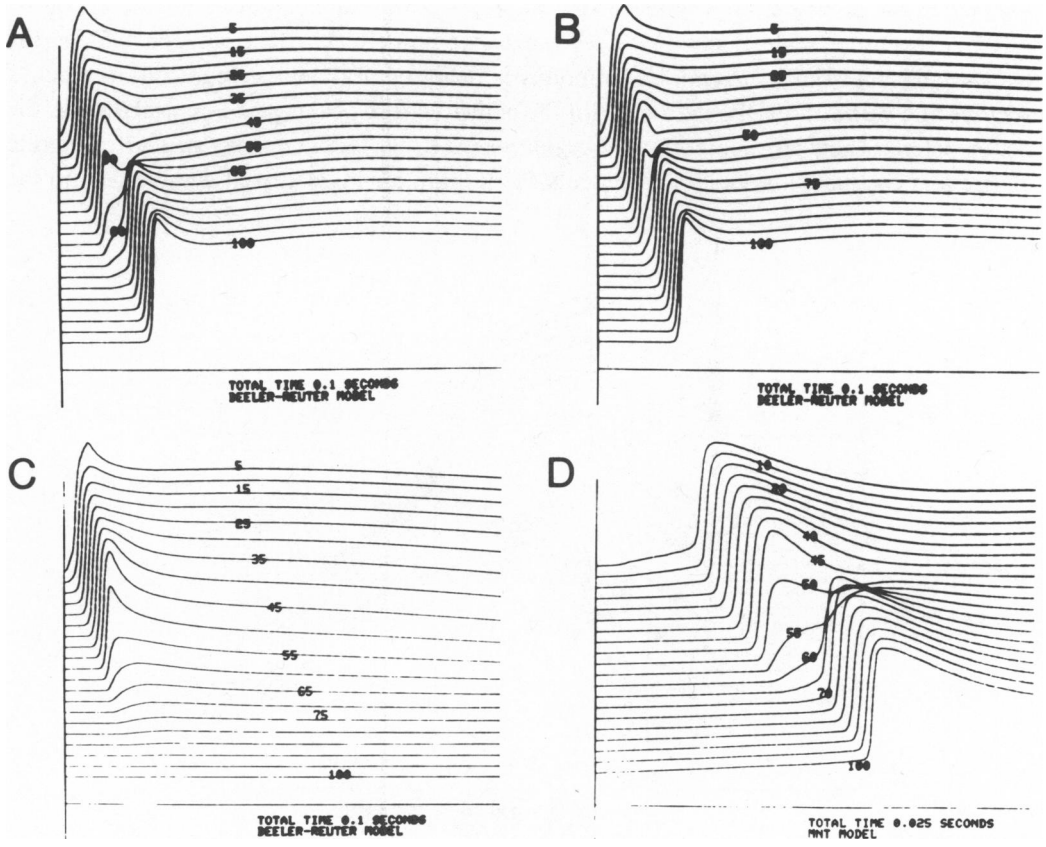

FIGURE 4 (*A*) A series of plots of voltage versus time for 20 segments (5, 10, 15 ... 100) for a 100-segment cable ($\Delta X = 62.5\ \mu m$) in which the BR model has $\bar{g}_{Na} = 0$ for segments 51–56. (*B*, *C*) Same as *A*, except that $\bar{g}_{Na} = 0$ for segments 51–54 (*B*) or 51–58 (*C*). (*D*) Same as *A* except that MNT membrane model was used and $\bar{g}_{Na} = 0$ for segments 50–60.

PAP characterized by slowing in the rate of rise and a decreased maximum amplitude as the action potential approaches the region of decreased excitability. There is delay of excitation in the region distal to the area where $\bar{g}_{Na} = 0$. When the distal region does initiate an action potential there is a second depolarization phase in the proximal region due to electrotonic coupling. These effects are more marked in part *A*, where the loss of excitability extends over a longer region; in part *C*, where the inexcitable region is even longer, there is a failure of propagation. Parts *A*, *B*, and *C* of the figure were done with BR model, whereas in part *D*, we show the results for the MNT model in a cable in which segments 50-60 had $\bar{g}_{Na} = 0$. Note that with the MNT model, propagation is successful over regions of depressed excitability longer than those which produced failure of propagation of the BR model.

Since, in these simulations, the region was not made completely passive (only $\bar{g}_{Na}$ was set to zero) it was of interest to see if an action potential could be initiated and propagated via the mechanism of the slow inward current. It was apparent that this was not the case at the normal resting potential since the threshold for the slow inward current was expected to be at about -40 mV. Therefore, we simulated a fiber which had a region in which not only was $\bar{g}_{Na}$ set to zero, but the fiber region was also depolarized. Fig. 5 shows the results for a 100 segment cable in which, for segments 51–100, $\bar{g}_{Na} = 0$ and the membrane is depolarized by $\sim$10 mV by using scale factors of 2 for the background sodium current and 0.5 for the background potassium current. The stimulus is delayed to allow the segments to reach a steady state value of depolarization. With the added feature of this small depolarization, the action potential now propagates into the region where $\bar{g}_{Na} = 0$ as the "slow response." The rate of rise and conduction velocity of segments 51–100 are much decreased with respect to the

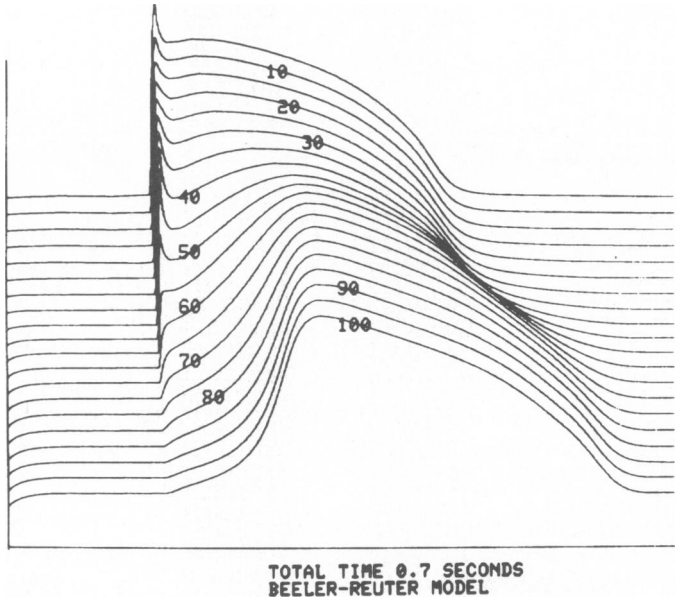

FIGURE 5 A series of plots of voltage versus time for 20 segments (5, 10, 15 . . . 100) for a 100-segment cable ($\Delta X = 62.5$ μm) in which the BR model for segments 51-100 was modified with $\bar{g}_{Na} = 0$ and a depolarization was produced by scaling the background Na current by 2.0 and scaling the background K current by 0.5.

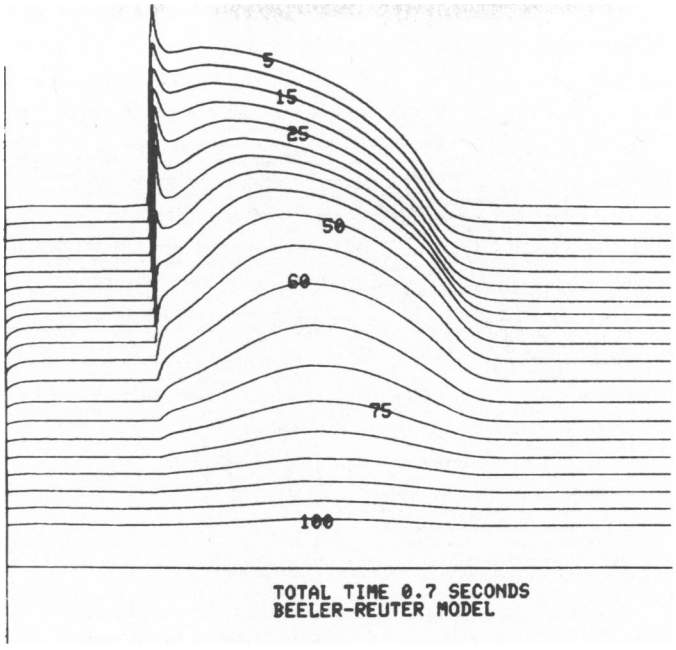

FIGURE 6 A series of plots of voltage versus time for 20 segments (5, 10, 15 . . . 100) for a 100-segment cable (ΔX = 62.5 μm) in which the BR model for segments 40–60 was modified with $\bar{g}_{Na}$ = 0 and a depolarization was produced by scaling the background Na current by 2.0 and scaling the background K current by 0.5.

normal segments 1–50. Conduction velocity of the "slow response" in this cable was 10% of the normal conduction velocity.

In the simulation just described, the region of the "slow response" extended from the middle of the fiber to the sealed end at segment 100. Fig. 6 shows the results of a simulation in which segments 40–60 had $\bar{g}_{Na}$ = 0 and were depolarized as before. In this case the slow response is initiated but fails to excite the normal region starting at segment 61. We had to increase the magnitude of the slow inward current by a factor of 3 in segments 40–60 to propagate from the region of the slow response into the normal region.

Spatial Inhomogeneities in Coupling Resistance

Fig. 7 illustrates several effects of regional changes in the coupling resistance. In part *A* the equivalent R_i is changed from the normal value of 200 Ω cm in segments 1–50 to 800 Ω cm for segments 51–100. The plots show the rising phases of the action potentials of segments 5–100 in increments of 5. The waveform of the PAP is unchanged, except at the transitional region, but the conduction velocity in segments 51–100 is decreased from 38 cm/s to 18 cm/s. For part *B*, the spatial increment of the simulation was reduced from 62.5 to 6.25 μm, and a coupling resistance of 20,000 Ω cm was used for segments 45–55. Propagation is successful, although there is a delay of ~ 15 ms in the region of high coupling resistance. In another simulation (not shown) using a cable identical to that of Fig. 7 *B* (except that the membrane model for all segments was modified to produce a plateau of smaller amplitude and duration,

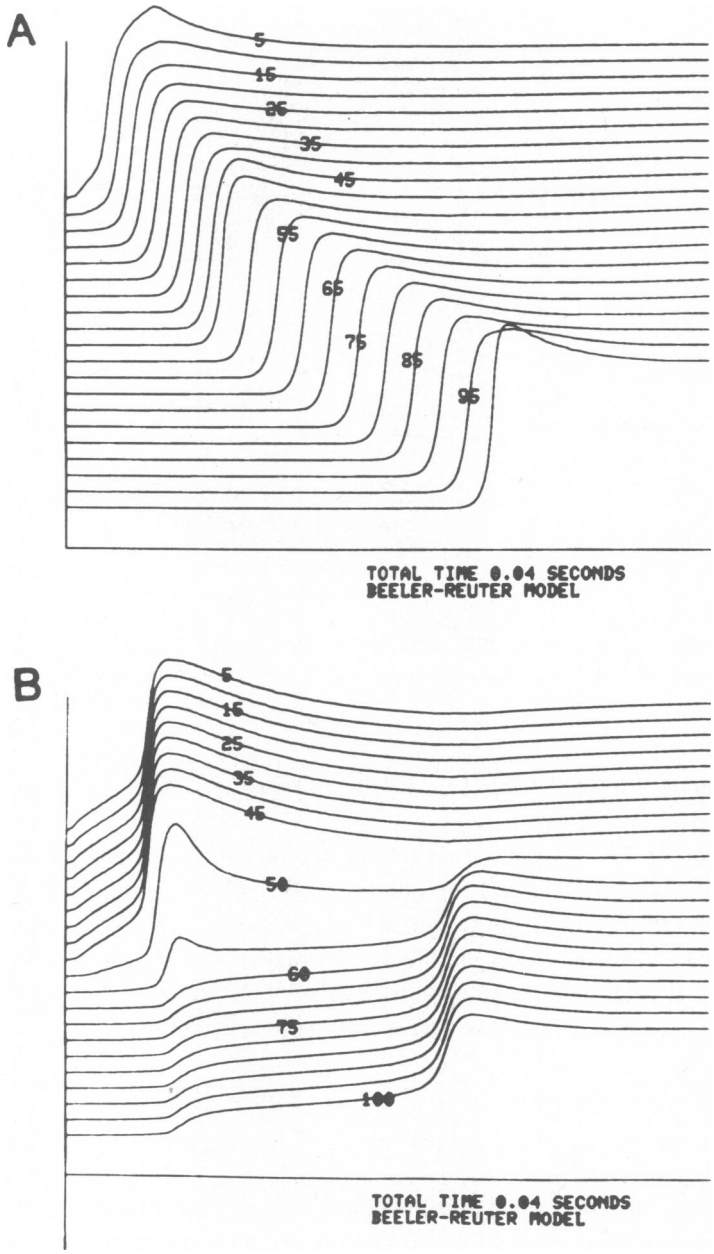

FIGURE 7 (*A*) A series of plots of voltage versus time for 20 segments (5, 10, 15 ... 100) for a 100-segment cable (ΔX = 62.5 μm) in which the internal resistivity is varied (R_i = 200 Ω cm for segments 1–50, R_i = 500 Ω cm for segments 51–100. (*B*) Same as *A*, except ΔX = 6.25 μm and R_i = 200 Ω cm for all segments except for segments 45–55, where R_i = 20,000 Ω cm.

scaling the slow inward current by 0.3), the action potential was blocked at the end of the region of high coupling resistance.

DISCUSSION

Validity of the Model

We emphasize several limitations in the applicability of these simulated results for understanding the mechanism of specific observed irregularities in cardiac action potential propagation. First, this model described how propagation is disturbed in a one-dimensional strand with regional inhomogeneities in membrane properties or intercellular coupling; there is no possibility in this model for longitudinal dissociation of the wavefront, or reentry via a circular loop. Second, the membrane models used are inexact representations of the electrical behavior of any specific type of cardiac cell. Third, the cable representation we used excludes effects of series resistance (resistance between the outer surface of the membrane and the extracellular bath ground), radial gradients in membrane potential or membrane properties, the additional capacitance of the transverse tubular system or intercellular clefts, or changes in ionic concentrations in the extracellular space. All of these limitations could be removed with specific quantitative assumptions to include these effects in the model description, but we feel that the basic propagational model presented here represents an integration of the primary determinants of cardiac action potential propagation and that the inclusion of other factors will have secondary, although very interesting, effects on propagation.

Homogeneous Cable

The simulations shown here are the first digital simulations of a propagating cardiac action potential using a complete model of the membrane properties. The unmodified BR model produced a PAP with a velocity (for a 5-μm cell diam) of 38 cm/s, a reasonable value for ventricle. One of the first questions considered in these simulations was the relationship between the MAP, as described by the BR model, and the PAP seen in these simulations for the homogeneous cable. The difference between the two should reflect the fact that for the PAP there is a voltage gradient along the cable, so that ionic current flow must not only change the potential of the local membrane, but also must support the potential difference between different sections of the cable. Since the steepest gradient exists between those areas not yet invaded by the action potential and those areas in which the rapid upstroke is occurring, the "loading" on the upstroke of the action potential should be greater than that for other parts of the waveform. As seen in Fig. 2 *B*, this is indeed the case. The MAP and PAP are essentially the same except for a slight difference in the upstroke.

Regional Changes in Action Potential Duration

The action potentials of central Purkinje fibers (those close to the AV node) are considerably longer than those of ventricular muscle. Mendez et al. (1969) found a gradual transition in duration from central Purkinje fibers to ventricular muscle cells. Also, ventricular muscle areas richly supplied with specialized conducting tissue had action potentials slightly longer than those where this tissue was absent. To determine if this gradual transition was the result of a gradual change in membrane properties or of the electrotonic interactions between the Purkinje fibers and the ventricular muscle cells, Mendez et al. (1969) performed the following

experiment. Recordings were made from central and peripheral Purkinje fibers before and after a transection was made in the area of the peripheral fibers (allowing enough time for "healing over" to take place). Before the transection, there was a marked difference in duration between the central and peripheral fibers. Thirty min after the transection, action potentials just proximal to the transection were prolonged and the differences in duration seen before the transection disappeared. Just distal to the transection, action potentials still had a short duration. These experiments are strikingly consistent with the simulations shown in Fig. 3. These simulations indicate that the presence of a gradual transition in electrical phenomena in closely coupled cells does not necessarily indicate a gradual transition in membrane properties. Despite the abrupt transition in membrane kinetic properties in the simulations, differences in membrane electrical properties between the two regions are obscured by the electrical coupling. This would suggest that electrical phenomena recorded from a cell are not necessarily indicative of the properties of that cell, but rather indicate some average of the electrical properties of that cell and the cells coupled to it.

It has often been suggested that extrasystoles and arrhythmias could be generated by the reactivation of fully repolarized cells by partially repolarized cells which had a longer action potential duration (Hoffman and Cranefield, 1964; Fowler, 1977). The transitions in duration which occur in areas of infarction have been considered likely sites for this "boundary current" types of reexcitation (Kupersmith et al., 1976; Kleber et al., 1978). Experimental support for this theory has been proposed to come from the work of Matsumura and Takaori (1959). These authors found that, at reduced calcium concentrations, preparations of the right atrium containing the sino-atrial node showed very long action potential durations in the nodal regions and repetitive firing of atrial fibers after each nodal action potential. Coupled beats in Purkinje-ventricular muscle preparations (Moore et al., 1964) and in sino-atrial node studies during vagal stimulation (Wallace and Daggett, 1964) have also been attributed to regional delayed repolarization. The phenomenon of rebound excitation has been described for "ventricular echo" beats resulting from ventricular stimulation with propagation in to the AV node and then a return to the ventricle (Rosenblueth, 1958; Moe et al., 1956), but it is not clear that this was not due to a dual pathway in the AV node instead of direct rebound excitation from adjacent regions. Rebound excitation has been seen in the squid axon when an abrupt regional change in action potential duration was created by perfusing the axon with teteaethylammonium (TEA) while an attached branch was perfused with a standard internal solution.[1] In this case, the large regional inhomogeneity in action potential duration produced rebound excitation and even, in some cases, prolonged repetitive firing at the transitional region. Repetitive firing has also been seen in skeletal muscle fibers in which the action potential has been prolonged by the application of TEA to the fiber (Hagiwara and Watanabe, 1955), but this may not represent true rebound excitation.

Rebound excitation could not be demonstrated in these simulations even with an abrupt fivefold difference in the action potential duration of the membrane model used for two adjacent regions. Associated increases in intercellular coupling resistance would allow for more abrupt regional changes in action potential duration, but would also decrease the magnitude of currents flowing intercellularly during the repolarization phase. It seems likely

[1]Ramon, F. Personal communication.

that rapid changes in coupling resistance (as a function of time and/or voltage) could lead to rebound excitation, but, in view of the lack of data for such assumptions, this was not further studied. Thus, it would seem that reexcitation by delayed repolarization in the Purkinje or ventricular system is unlikely to occur because of the nature of the repolarization process in these tissues. The membrane resistance remains high during the plateau and repolarization phase (in contrast to nerve and skeletal muscle) and therefore the effective space constant remains large, enabling electrotonic interactions to obscure the transitional effects by prolonging the action potential duration in the region with inherently short action potential duration and shortening the action potential in the region with inherently long action potential duration. This same conclusion was reached by Mendez et al. (1969) on the basis of their experiments previously described.

As has been discussed, action potential duration varies continuously along the specialized conduction system. From the bundle branches to the central Purkinje fibers, the duration increases. As the specialized conduction system approaches the ventricular cells, the duration decreases. The region of longest action potential duration also coincides with the region of longest refractory period. This area had been termed a "gate," and has been thought to function as a determinant of the functional refractory period of the Purkinje-ventricular system (Myerburg et al., 1970), blocking premature impulses from above and below this level. This idea has been questioned for the in vivo conduction system, since these experiments were done in vitro with only part of the conduction system (Lazzara et al., 1975). Fig. 3 *B* shows the simulation of the blocking of a premature action potential propagating from an area of short action potential duration to an area of longer action potential duration. When the delay for the second action potential was increased, it propagated further along the fiber. This is similar to experiments done by Myerburg et al. (1970) and by Mendez et al. (1969) in which, by increasing the delay between stimuli applied to papillary muscle, block could be caused to occur at a higher level in the Purkinje system.

Inexcitability

Depressed conduction has been studied experimentally by several techniques, including a "blocking current" (Wennemark et al., 1968), external pressure or focal cooling (Downer and Waxman, 1976), and locally high potassium concentration (Cranefield et al., 1971). Simulations of depressed conduction have been done using a partial model of the cardiac action potential (Lieberman et al., 1973) and by analytical solutions for special boundary conditions (Terry et al., 1972). One problem in dealing experimentally with depressed conduction is that it is difficult to alter one tissue parameter independently of others, and to know the extent to which this parameter has been altered. Nonetheless, these different techniques produced remarkably similar effects on the action potential waveforms. Proximal to the area of depression, notches were observed after the spike of the action potential, with the termination of the notch coincident with the rising phase of the action potential distal to the area of depression. These distal action potentials arose from a small prepotential. These characteristics are readily seen in the simulations in Figs. 4–7, using a decreased $\bar{g}_{Na}$ or a change in longitudinal impedance to create a "depressed" area. In the simulations, the changes in the PAP waveforms are caused by the electrical interactions between the two regions on each side of the "depressed" area. As the action potential propagates toward the area of depression,

current will flow from the active area to areas not yet active. In the normal fiber, this causes only a slight load on the action potential (as seen in the difference between the MAP and the PAP for the homogeneous cable). In an area of depression, however, the current must flow into this area and the distal area as well, to propagate through the depressed region. Thus a much larger than normal electrical load is imposed on the propagating action potential. This load leads to an early partial repolarization of the action potential proximal to the area of depression, producing the early part of the notch. This flow of current slowly charges the membrane in the depressed area and the distal area, causing the observed prepotential. When the active area distal to the area of depression reaches threshold and initiates an action potential, the electrical load on the proximal regions is removed and there is a reversed flow of current which terminates the notch. In the simulations in which the axial resistance is changed, the critical region for successful propagation is the abrupt transition from high to low axial resistivity. In this region, an action potential propagating from an area with a short length constant must activate an action potential in an area with a long length constant. This means that there is again an effectively increased electrical load imposed on the propagating action potential, and the effects on the PAP are similar to those seen for a region of decreased excitability.

The maximum delay obtainable at a depressed region will be determined by the threshold characteristics of the region distal to the area of depression. We examined the threshold characteristics of a homogeneous cable with the BR membrane model by calculating a stimulus strength-duration relationship for stimulation at a single segment. The curve reached the rheobase level for durations as large as 30 ms with no action potential generated if the stimulus was slightly lower. This would indicate that a delay of no longer than ~30 ms could be expected at a region of depression, and we could not generate a longer delay in the model without propagation failure. This result must be cautiously considered, however, since the most arbitrary part of both the MNT and the BR models is their description of the fast sodium current which would be the primary determinant of threshold characteristics.

Since the electrical load imposed on a propagating action potential is determined by the length of the depressed region, there should be a critical length of the depressed region for which propagation is blocked (Fig. 4). This critical length is not determined only by the amount of electrotonic attenuation along the depressed region, since a membrane model with more inward current (e.g., MNT compared with BR) will propagate successfully through a length of depressed region long enough to block the "weaker" action potential. It is especially interesting to note the marked spike-like appearance of the action potentials in the area proximal to the region of propagation block. In normal homogeneous propagation, as discussed before, the spike of the PAP is diminished (with respect to the MAP) while the plateau is virtually unchanged. This is due to the large voltage gradient seen by the propagating spike. Here, however, in the case of inhomogeneous propagation, although both the spike and the plateau are diminished in amplitude, the plateau is relatively more affected, leading to an early repolarization. The difference in the relative effects in the two situations is due to the resistance changes during the cardiac action potentials. During the spike, the cable is relatively uncoupled because of the high membrane conductance. The plateau phase is more susceptible to the loading effects of cable inhomogeneities because of the high membrane resistance during this phase of the action potential. This spike-like shortening of the action

potential has been noted by several investigators (e.g., Sasyniuk and Mendez, 1971) in regions proximal to propagation failure both at the Purkinje-ventricular muscle junction and in the AV node. This abbreviated action potential was found to have a corresponding short refractory period and could lead in some cases to early reentrant activity in Purkinje fibers. This effect might be responsible for the spike-like action potentials seen by Churney and Oshima (1964) in small bundles of fibers from amphibian hearts or small cut pieces of dog ventricles.

Since the charge necessary to bring a membrane region to threshold comes from the longitudinal current, and since this current depends on the potential differences between the active region and the inactive region, a decrease in the action potential amplitude or duration would decrease the time integral of the longitudinal current and thus might cause failure of propagation to occur if the total charge transferred were reduced. This type of mechanism has been demonstrated experimentally in nerve by Westerfield et al. (1978), who showed that the temperature dependent failure of action potential propagation at branch points in squid axons is closely related to the change in duration of the action potential with temperature. It seems unlikely that a decrease in the duration of the cardiac action potential alone would lead to propagation failure at inhomogeneous regions, since the maximum expected delay is much shorter than the normal duration. However, the same effect of decreasing the time integral of longitudinal current flow (the charge transferred) can be obtained by a decrease in the plateau amplitude. As discussed in Results, block occurred in the simulation of Fig. 7 *B* if the plateau phase of the action potential was decreased in amplitude and shortened in duration. This effective decrease in the safety factor for action potentials with decreased duration and plateau amplitude may be important in understanding the changes in propagation of premature beats and frequency dependent failure at various regions of the heart. A premature beat with smaller amplitude and shorter duration may not be able to support the electrical load of an area of depression, and propagation block could result. Similarly, the change in waveform caused by a change in stimulation frequency could lead to alternating block.

Transitional Cells

Many electrophysiological studies have shown distinctive action potential shapes to occur at the junction between different regions in the heart. These include areas in the AV node (Alanis and Benitez, 1967) and between Purkinje fibers and ventricular muscle cells (Mendez et al., 1970). These action potentials include characteristic notches in the depolarization or early repolarization phases. Of special interest is that the termination of the notch occurs simultaneously with the rising phase of the action potential in cells distal to the transitional regions. The cells in which these action potentials have been recorded have been referred to as transitional cells (Alanis and Benitez, 1967). In the case of the cells at the Purkinje-myocardial junction, the transitional cells appear to have some distinct anatomical features (Martinez-Palomo et al., 1970). As a result of these simulations, it is not surprising that cells transitional in electrical behavior between two coupled areas exist. In fact, for two regions electrically coupled, it would be impossible for transitional cells not to appear, and the determination of truly distinct transitional cells can not be made on an electrophysiological basis.

Two theories have been proposed for the notches and delays seen at the Purkinje-

myocardial junction. Martinez-Palomo et al. (1970) reported a paucity of intercellular junctions between the transitional cells. This would be equivalent to our simulation in which a region of the cable had a high coupling resistance. A second theory was proposed by Mendez et al. (1970). This theory (the "funnel" hypothesis) proposes that the functional geometry at the Purkinje-myocardial junction changes from a cable-like system at the Purkinje level to a three-dimensional syncytium at the ventricular level, thus producing an increase in the electrical load seen by the propagating action potential. Mendez et al. (1970) found that, if excitability of the preparation was generally lowered by exposure to high concentrations of potassium, conduction was blocked from Purkinje fibers to ventricular muscle before it was blocked in the other direction. Similar results were reported by de la Fuente et al. (1971) on a preparation of atrial muscle consisting of a large mass of tissue connected to a small mass of tissue by a narrow isthmus. Conduction across the isthmus failed when it proceeded from the small mass to the large mass, while conduction in the reverse direction was maintained. While our simulations cannot be used to distinguish between the several mechanisms proposed for the propagational changes seen at the Purkinje-ventricular muscle junction, they do illustrate the similarity of the effects of either mechanism and relate these effects to a changing electrical load seen by the propagating action potential.

The Slow Response

As has been discussed previously, propagated action potentials have been observed in Purkinje strands under conditions in which the fast sodium current is largely absent, and this has been attibuted to propagation via the mechanism of the slow inward current. It is of interest that the BR model, which was not constructed to model this response, will propagate a "slow response" action potential under the conditions of $\bar{g}_{Na} = 0$ and a resting membrane polarization. The requirement of a depolarization from the resting potential is probably related to the large difference between the normal resting potential and the threshold for activation of the slow inward current. Note that the change in the background currents we used to generate the depolarization would also tend to increase the membrane resistance in the resting state, which would also favor the propagation of the "slow response." Experimentally, it has been found by Carmeliet and Vereecke (1969) that fibers exposed to high potassium and epinephrine are very difficult to stimulate. Cranefield et al. (1971) used a technique of application of high potassium by an agar patch that enabled them to evoke the slow response by the propagation of a normal action potential into the region of the high potassium concentration. It has also been frequently observed that block occurs in the segment exposed to the high potassium agar, which is consistent with our simulations, indicating that propagation was marginal and the action potential was not able to propagate from the "slow response" region in to a normal region.

It must be emphasized, however, that the simulations are different from the experimental arrangement in at least two ways: (*a*) The transition between regions is gradual in the experiments due to diffusion of the potassium, while in these simulations we used abrupt boundaries. (*b*) A simple one-dimensional cable may not be an accurate representation of a fiber exposed to high potassium and epinephrine. Although the Purkinje fiber is long and thin and resembles a right circular cylinder, it is not a simple system. A bundle of Purkinje fibers 1 mm in diameter can contain from 5 to 15 fibers electrically connected in a complicated

manner by gap junctions and branches (Sommer and Johnson, 1968). There is evidence that under depolarized conditions there may be longitudinal dissociation among the cells (Anderson et al., 1970; Myerburg et al., 1976). These additional complexities may be required to reproduce some phenomena which we did not see in our simulations, including the return of an action potential from a potassium-agar treated region into a normal region (Wit et al., 1972).

We thank Craig Hobbs for his assistance in computer programming and The University of Iowa for the generous allotment of computer time for this project.

This work was supported by National Institutes of Health grants HL22562 and NS15350 to Dr. Joyner.

Received for publication 7 April 1980.

REFERENCES

ALANIS, J., and D. BENITEZ. 1967. Transitional potentials and the propagation of impulses through different cardiac cells. *In* Electrophysiology and Ultrastructure of the Heart. T. Sano, V. Misuhira, and K. Matsuda, editors. Grune & Stratton, Inc., New York. 153–177.

ANDERSON, G. J., K. GREENSPAN, J. P. BANDURA, and C. FISCH. 1970. Asynchrony of conduction within the canine specialized Purkinje fiber system. *Circ. Res.* **27**:691–703.

ATWELL, D., and I. COHEN. 1977. The voltage clamp of multicellular preparations. *Prog. Biophys. Mol. Biol.* **31**:201–245.

BEELER, G. W., and H. REUTER. 1977. Reconstruction of the action potential of myocardial fibres. J. Physiol. **268**:177–210.

BRILL, M. H., S. G. WAXMAN, J. W. MOORE and R. W. JOYNER. 1977. Conduction velocity and spike configuration in myelinated fibers. *J. Neurol. Neurosurg. Psychiatry.* **40**:769–774.

CARMELIET, E., and J. VEREECKE. 1969. Adrenaline and the plateau phase of the cardiac action potential. *Pfluegers Arch. Eur. J. Physiol.* **313**:300–315.

CHALLICE, C. E. 1971. Functional morphology of the specialized tissues of the heart. *Methods Achiev. Exp. Pathol.* **5**:121–172.

CHURNEY, L. and H. OSHIMA. 1964. Effect of tissue mass on shape of action potential recorded from excised dog ventricle. *Fed. Proc.* **23**:117.

CLERC, L. 1976. Directional differences of impulse spread in trabecular muscle from mammalian heart. *J. Physiol. (Lond.).* **255**:333–346.

COOLEY, J. W., and F. A. Dodge, Jr. 1966. Digital computer solutions for excitation and propagation of the nerve impulse. *Biophys. J.* **6**:583–599.

CRANEFIELD, P. F., H. O. KLEIN, and B. F. HOFFMAN. 1971. Conduction of the cardiac impulse. 1. Delay, block and one-way block in depressed Purkinje fibers. *Circ. Res.* **28**:199–219.

CRANK, J., and P. NICHOLSON. 1947. A practical method for numerical evaluation of solutions of partial differential equations of the heat-conduction type. *Proc. Camb. Philos. Soc. (Math. Phys. Sci.).* **43**:50–67.

DECK, K. A., R. KERN, and W. TRAUTWEIN. 1964. Voltage clamp technique in mammalian cardiac fibers. *Arch. Gesamte. Physiol. Mens. Tiere (Pfluegers).* **280**:50–62.

DE LA FUENTE, D., B. I. SASYNIUK, and G. K. MOE. 1971. Conduction through a narrow isthmus in isolated canine atrial tissue. A model of the WPW syndrome. *Circulation.* **46**:803.

DE MELLO, W. C. 1976. Influence of the sodium pump on intercellular communication in heart fibres: effect of intracellular injection of sodium ion on electrical coupling. *J. Physiol. (Lond.).* **263**:171–197.

DOWNER, E., and M. B. WAXMAN. 1976. Depressed conduction and unidirectional block in Purkinje fibers. *In* The Conduction System of the Heart. H. J. J. WALLENS, K. I. LIE, and M. J. JANSE, editors. LEA & FEBIGER, Philadelphia. 393–409.

FOWLER, N. W. 1977. Cardiac arrhythmias: diagnosis and treatment. Harper & Row, Publishers, Inc., New York. 236.

GOLDSTEIN, S., and W. RALL. 1974. Changes of action potential shape and velocity for changing core conductor geometry. *Biophys. J.* **14**:731.

HAGIWARA, S., and A. WANTANABE. 1955. The effect of tetraethylammonium chloride on the muscle membrane examined with an intracellular microelectrode. *J. Physiol. (Lond.).* **129**:513–527.

HODGKIN, A. L, and A. F. HUXLEY. 1952. The components of membrane conductance in the giant axon of Loligo. *J. Physiol. (Lond.).* **116**:473–496.

HOFFMAN, B. F., and P. F. CRANEFIELD. 1964. Physiological basis of cardiac arrhythmia. *Am. J. Med.* **37**:670–684.

JOHNSON, E. A., and M. LIEBERMAN. 1971. Heart: excitation and contraction. *Annu. Rev. Physiol.* **33**:479–532.

JOYNER, R. W., F. R. RAMON, and J. W. MOORE. 1975. Simulation of action potential propagation in an inhomogeneous sheet of electrically coupled excitable cells. *Circ. Res.* **36**:654–661.

JOYNER, R. W., R. M. WESTERFIELD, J. W. MOORE, and N. STOCKBRIDGE. 1978. A numerical method to model excitable cells. *Biophys. J.* **22**:155–170.

KLEBER, A. G., M. J. JANSE, and D. DURROR. 1978. Mechanism and time course of S-t and T-Q segment changes during acute regional myocardial ischemia in the pig heart determined by extracellular and intracellular recordings. *Circ. Res.* **42**:603–613.

KUPERSMITH, J., H. SHIANG, R. W. LITWAK, and M. V. HERMAN. 1976. Electrophysiological and antiarrhythmic effects of propranolol in canine acute myocardial ischemia. *Circ. Res.* **38**:302–307.

LAZZARA, R., N. EL-SHEFIF, and B. J. SCHERLAG. 1975. Disorders of cellular electrophysiology produced by ischemia at the canine his bundle. *Circle Res.* **36**:444–454.

LIEBERMAN, M., J. M. KOOTSEY, E. A. JOHNSON, and T. SAWANOBORI. 1973. Slow conduction in cardiac muscle: a biophysical model. *Biophys. J.* **13**:37–55.

LIEBERMAN, M., T. SAWANOBORI, J. M. KOOTSEY, and E. A. JOHNSON. 1975. A synthetic strand of cardiac muscle: its passive electrical properties. *J. Gen. Physiol.* **65**:527–550.

MARTINEZ-PALOMO, A., J. ALANIS, and D. BENITEZ. 1970. Transitional cardiac cells of the conductive system of the dog heart. *J. Cell Biol.* **47**:1–17.

MATSUMURA, M., and S. TAKAORI. 1959. The effects of drugs on the cardiac membrane potentials in the rabbit. II. Auricular muscle fibers and the sino-atrial node. *Jpn. J. Pharmacol.* **8**:143–150.

MCALLISTER, R. E., D. NOBLE, and R. W. TSIEN. 1975. Reconstruction of the electrical activity of cardiac Purkinje fibers. *J. Physiol. (Lond.).* **251**:1–59.

MENDEZ, C., W. J. MUELLER, and X. URGUIAGA. 1970. Propagation of impulses across the Purkinje fiber-muscle junctions in the dog heart. *Circ. Res.* **26**:135–150.

MENDEZ, D., W. J. MUELLER, J. MEREDITH, and G. K. MOE. 1969. Interaction of transmembrane potentials in canine Purkinje fibers and at Purkinje fiber-muscle junctions. *Circ. Res.* **24**:361–372.

MOBLEY, B. A., and E. PAGE. 1972. The surface area of sheep cardiac Purkinje fibres. *J. Physiol. (Lond.).* **220**:547–563.

MOE, G. K., J. B. PRESTON, and H. BURLINGTON. 1956. Physiologic evidence for a dual A-V transmission system. *Circ. Res.* **4**:357–375.

MOE, G. K., W. C. RHEINBOLDT, and J. A. ABILDSKOV. 1964. A computer model of atrial fibrillation. *Am. Heart J.* **67**:200–220.

MOORE, E. N., H. T. MORSE, and H. L. PRICE. 1964. Cardiac arrhythmias produced by catecholamines in anesthetized dogs. *Circ. Res.* **15**:77–82.

MOORE, J. W., F. RAMON, and R. W. JOYNER. 1975. Axon voltage-clamp simulations. I. Methods and tests. *Biophys. J.* **15**:11.

MOORE, J. W., R. W. JOYNER, M. H. BRILL, S. G. WAXMAN, and M. NAJARO-NOA. 1978. Simulations of conduction in uniform myelinated fibers. *Biophys. J.* **21**:147–160.

MYERBURG, R. F., J. W. STEWART, and B. F. HOFFMAN. 1970. Electrophysiological properties of the canine peripheral A-V conducting system. *Circ. Res.* **26**:361–378.

MYERBURG, R. J., H. GELBAND, and A. CASTELLANOS. 1976. Electrophysiology of endocardial intraventricular conduction: the role and function of the specilized conducting system. *In* The Conduction System of the Heart. H. J. Wellens, K. I. Lie, and M. J. Janse, editors. Lea & Febiger, Philadelphia. 336–359.

POLLACK, G. H. 1976. Intercellular coupling in the atrioventricular node and other tissues of the rabbit heart. *J. Physiol. (Lond.).* **255**:275–298.

ROSENBLUETH, A. 1958. Ventricular "echoes." *Am J. Physiol.* **195**:53–60.

ROUGIER, O., G. VASSORT, and R. STÄMPFLI. 1968. Voltage clamp experiments of frog atrial heart muscle with the sucrose gap technique. *Pfluegers Arch. Eur. J. Physiol.* **301**:91–108.

SASYNIUK, B. I., and C. MENDEZ. 1971. A mechanism for re-entry in canine ventricular tissue. *Circ. Res.* **28**:3–15.

SCHANNE, O. F., and E. RUIZ-CERETTI. 1978. Impedence measurements in biological cells. John Wiley & Sons, Inc., New York. 430.

SCHAUF, C. L., and F. A. DAVIS. 1974. Impulse conduction in multiple sclerosis. *J. Neurol. Neurosurg. Psychiatry.* **37**:152–161.

SOMMER, J. R., and E. A. JOHNSON. 1968. Purkinje fibers of the heart examined with the peroxidase reaction. *J. Cell Biol.* **37**:570–574.

TERRY, F. H., J. R. WENNEMARK, and D. A. BRODY. 1972. Numerical simulation of conduction delay in blocked Purkinje tissue. *Circ. Res.* **31**:53–64.

VAN CAPELLE, V., and M. J. JANSE. 1976. Influence of geometry on the shape of the propagated action potential. *In* The Conduction System of the Heart. H. J. WELLENS, K. I. LIE, and M. J. JANSE, editors. Lea & Febiger, Philadelphia.

WALLACE, A. B., and W. M. DAGGETT. 1964. Atrial re-excitation: "the echo phenomenon." *Am. Heart J.* **68**:661–666.

WEIDMAN, S. 1970. Electrical constants of trabecular muscle from mammalian heart. *J. Physiol. (Lond.).* **210**:1041–1054.

WEINGART, R. 1975. Electrical uncoupling in mammalian heart muscle induced by cardiac glycosides. *Experientia (Basel).* **31**:715.

WENNEMARK, J. R., V. L. RUESTA, and D. A. BRODY. 1968. Microelectrode study of delayed conduction in the canine right bundle branch. *Circ. Res.* **23**:753–769.

WESTERFIELD, R. M., R. W. JOYNER, and J. W. MOORE. 1978. Temperature-sensitive conduction failure at axon branch points. *J. Neurophysiol. (Bethesda).* **41**:1–8.

WIENER, N., and A. ROSENBLUETH. 1946. Conduction of impulses in cardiac muscle. *Arch. Inst. Cardiol. Mex.* **16**:205–265.

WIT, A. L., B. F. HOFFMAN, and P. F. CRANEFIELD. 1972. Slow conduction and reentry in the ventricular conducting system. I. Return extrasystole in canine Purkinje fibers. *Circ. Res.* **30**:1.

WOODBURY, J. W., and W. E. CRILL. 1961. On the problem of impulse conduction in the atrium. *In* Nervous Inhibition, Proceedings of an International Symposium. Pergamon Press, Inc., Elmsford, N.Y. 124–135.